

Nonlinear Stability Analysis of Elastic High Strength Steel Tubes Under Global Bending

Ngalle Itoumbou Christina Joyce, Lei Chen, Kapnang Franky

School of Civil Engineering, Henan University of Technology, Zhengzhou, PR China

Email address:

christajoy@yahoo.com (N. I. C. Joyce), chenleihe2008@163.com (Lei Chen), frankykapnang@gmail.com (K. Franky)

To cite this article:

Ngalle Itoumbou Christina Joyce, Lei Chen, Kapnang Franky. Nonlinear Stability Analysis of Elastic High Strength Steel Tubes Under Global Bending. *American Journal of Civil Engineering*. Vol. 10, No. 2, 2022, pp. 64-69. doi: 10.11648/j.ajce.20221002.15

Received: March 20, 2022; **Accepted:** April 20, 2022; **Published:** April 28, 2022

Abstract: A recent computational study has found unique zones of stability behaviour in elastic High-strength steel tubes under global bending with different geometrical lengths. A situation under which the most compressed fiber approaches the buckling stress for uniform axial compression is the initial estimation of elastic buckling strength in bending. Cylinders with sufficient length develop a fully developed ovalization of the cross-section and fail by local buckling around the Brazier prediction. Under global bending regimes, typical buckles are fairly modest and extend across a very tiny region, accompanied by global bending extending the crucial value. The situation under which the major compressed fiber approaches the buckling stress for compression bending is the initial estimate of the elastic buckling strength in bending. In this study, the nonlinear behavior of short to long tubes under global bending is studied, with specific and different dimensions, radius-to-thickness ratios, and boundary conditions according to Europe an Standard 1993-1-6. Both the crucial buckling Eigenmode and the geometrically nonlinear elastic analysis are investigated. Because of a buckling stress state dominated by local harmony bending, it is confirmed that the cylinder length takes part in a crucial part in finding this behavior. A failure behavior of this type of material is then going to be investigated.

Keywords: High Steel Strength, Ovalization, Buckle, Non-uniform, Elastic, Post-buckling, Global Bending

1. Introduction

Structural steel was first used in the nineteenth century, then some tubes under global bending were also studied [1-4]. Because of its high strength, stable material properties, and rapid, high-quality construction, its potential as a structural material was quickly recognized [5]. The minimum yield strength for structural steel grades was 220 N/mm² for bridges and 240 N/mm² for buildings [6]. The growing market needs to be combined with advances in materials science led to the introduction of higher strength structural steels in the construction industry. The steel industry has developed structural steels with yield strengths exceeding 690 N/mm², commonly referred to as high-strength steels (HSS).

This problem has been the subject of detailed analytical treatments for more than a century. In fact, were among the first to investigate the nonlinear behavior of long tiny-walled circular cross-sectionals in bending to describe how classic linear beam theory wasn't able to reproduce the occurrence of ovalization [7, 8].

Brazier's simple analysis, which used an extremely long cylinder as a structural member including a presumed nonlinear displacement field, has demonstrated that gradual ovalization of the cross-sectional under deformation led directly to a boundary point destabilization at a crucial value, today identified as the Brazier moment.

Seide and Weingarten's crucial bending moment for short tubes with minor ovalization is about double Brazier's maximum bending moment for an endlessly long cylindrical shell with Brazier ovalization of the cross-section [9]. Therefore, with in case of medium long tubes, the structure's reaction comprises a combination of ovalization and bifurcation instability. The degree of ovalization of the cross-section grows with increasing length, but the Brazier critical ovalization is not reached, and the elastic critical bending moment decreases slowly towards the value corresponding to an infinitely long cylinder. Lot of study has already been introduced on the connection between the ovalization instability and the bifurcation instability for cylindrical shells in bending. Axelrad first viewed the

interaction of the two kinds of instability [10] mentioned above, and then introduced the effect of ovalization as a pre-buckling deformation on local buckling. Local buckling was expected to occur when the maximum compressive stress at the most compressed fibres achieved the critical point for uniform compressed tubes with a radius equivalent to the global radius of the ovalized shell at the "crucial" point.

The ABAQUS fine elements program was used in this study to compute and extract results for the analysis on different lengths, and to examine the numerical nonlinear stability analysis of elastic strength steel tubes under global bending's behavior.

2. Analysis and Numerical Result

2.1. Geometrical, Load, and Material Properties

All incrementations and calculations analyses were elaborated through ABAQUS finite analysis software [11]. Because it is difficult to define the post-buckling deformed shape in a unique and repeatable manner according to its form changes progressively, different geometries were used with radius to thickness ratios with the range of $R/t=10\sim500$, and the length to radius ratios and a thickness of 1mm throughout the work [12, 13].

To better compare results, similar boundary conditions were applied to both shell ends in all analyses. The axial translational degrees of freedom and the global rotational degrees of freedom were both unconstrained, while all other degrees of freedom were unconstrained. Due to symmetry, the whole shell model was used and the boundary conditions were set at two edges of the shell.

This research focuses on the strength of perfectly elastic cylinders subjected to global bending but also his stability. To reach our goal, the linear buckling mode analyses (LBA) for appropriate structures were first performed to obtain the reference buckling moment M_{LBA} .

The M_{LBA} was then imposed at both ends to perform geometric nonlinear analysis (GNA) to determine the bifurcation and the limit load point for the perfect structure.

The first dimensionless reference moment was normalized by

$$k_1 = M_{GNA} / M_{LBA} = M / M_{cr} \quad (1)$$

The Brazier ovalization limit moment is expressed as:

$$M_{Braz} = 0.987 \left(\frac{E}{\sqrt{1-\nu^2}} \right) t^2 r \cong 1.015 E t^2 r \quad (2)$$

The crucial elastic bending moment is expressed as:

$$M_{cr} = 1.814 \left(\frac{E}{\sqrt{1-\nu^2}} \right) t^2 r \cong 1.866 E t^2 r \quad (3)$$

Then the second reference dimensionless moment was normalized by

$$k_2 = M_{GNA} / M_{Braz} = M / M_{Braz} \quad (4)$$

Dimensionless length are both expressed as:

$$\Omega = L t^{1/2} / r^{3/2} \quad (5)$$

$$\omega = L / \sqrt{r t} \quad (6)$$

With r as radius, t as thickness, E as modulus of elasticity, L as length and ν as Poisson's ratio [4, 13, 14]. The shell has been made of an isotropic material with $E=2.0E5$ MPa and $\nu=0.235$.

2.2. Model of Shell Elements

The general S4R5 element was used. To capture the local bending and buckling modes, a finite element with element size of $0.25\sqrt{rt}$ length elements only was used [15].

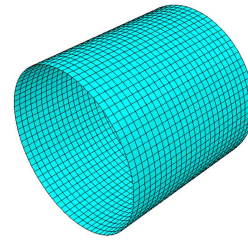


Figure 1. The mesh division of cylindrical shell.

2.3. Buckling Strength Predictions

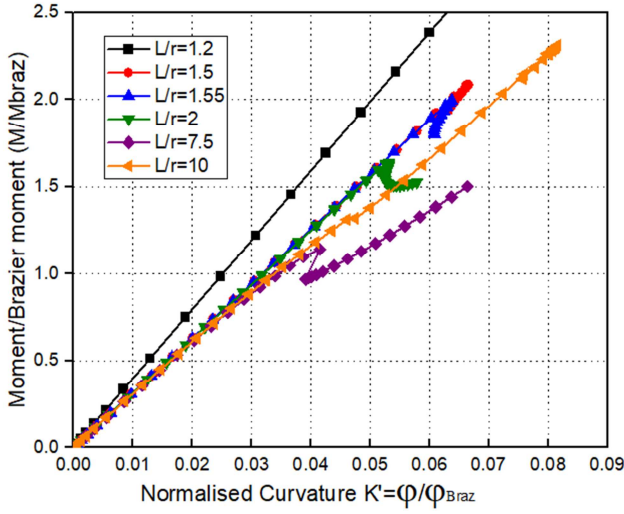
Here are studied tubes with a constant $r/t = 10$ with various linear measure. The dimensionless moment-curvature curves for tubes with the same ratio $r/t = 10$ are visible in Figure 2. The value of the moment in Figure 2a is normalized by M_{cr} (Eq. (7)) as $k_1 = M/M_{cr}$. The curvature is expressed as $k = \varphi/\varphi_{cr}$, whit φ as the main curvature along the tube and φ_{cr} is obtained based on the linear bending theory:

$$\varphi_{cr} = \frac{t}{r^2 \sqrt{3(1-\nu^2)}} \quad (7)$$

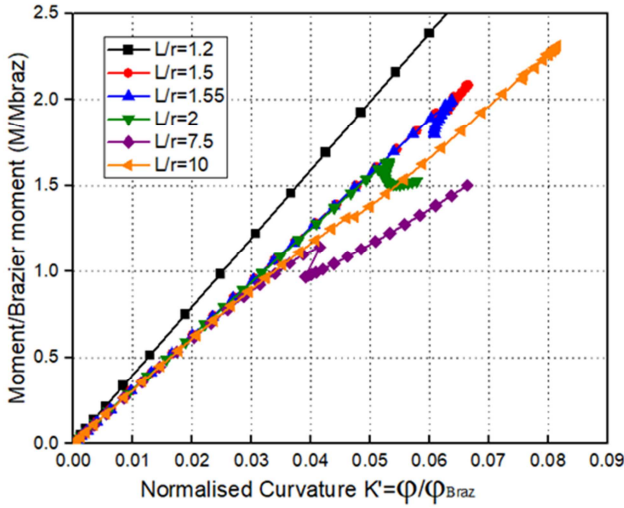
Regarding very tiny tubes ($L/r = 1.2$), the buckle is well restrained by the boundary conditions at two ends, and the crucial bending moment may exceed M_{cr} , and the dimensionless moment parameter m can reach a large value at the limit point.

When L/r becomes bigger, as $L/R=1.55$ and 2 for instance, bifurcation buckling occurs at a moment of $0.94 M_{cr}$ and $0.81 M_{cr}$ individually. The strength is limited by bifurcation buckling with a steep post-buckling fall, quickly followed by a recovery (in Figure 2a). The value of the limit moment is close to M_{cr} , suggesting that the critical bending stress for a cylinder under a uniform bending moment is close to the crucial stress for a tube. The buckling strength is unaffected by the border condition. According to linear bending theory, the curvature at the critical load is the same. According to Seide and Weingarten's approach, the critical bending moment for a tube with dimensional characteristics in a proper scope may be approximated. With a gradual increase of L/r (Figure 2a), the crucial bending moment appear to be less compare to M_{cr} , suggesting that the ovalization of the cross-sectional begins to considerably impact the buckling strength. Because of that ovalization, the local radius of curvature of the material

increases, as a result of a decrease in critical bending moment.



(a)



(b)

Figure 2. Dimensionless moment curvature-curves ($R/t=10$).

As L/r increases, the impact of ovalization of cross-sectional on the buckling strength becomes much valuable. The buckling behavior is a coupling among the ovalization of the cross-sectional and the formation of thin-wavelength bifurcation buckles. For bigger values of L/r , bifurcation buckling yields a more abrupt post-buckling falls (Figure 5), and determining that the post-buckling way is far more difficult to detect. While L/r 's value is more sufficient (Figure 3), the crucial bending moment is extremely near to an extremely long tube.. The bifurcation buckling point appears right before the snap-through buckling point in these cylinders. Buckling happens relatively locally, and the buckle's half wavelength is rather short, making the post-buckling path difficult to follow. The same moment-curvature curves can alternatively be shown in Figure 2b. Here the value of the moment is normalized by the Brazier moment as k_2 (Eq. (4)). The curvature is normalized as $k' = \phi / \phi_{Braz}$, where ϕ_{Braz} is When M_{Braz} is achieved, the curvature is obtained using the

linear bending hypothesis as:

$$\phi_{Braz} = 0.314 \frac{t}{r^2 \sqrt{1-\nu^2}} \quad (8)$$

According to Figure 2b, at the moment k_2 almost equal to 1, meaning critical moment approaches M_{Braz} and so the bifurcation buckling occurs with Brazier critical ovalization of the cross-section. When $k_2 > 1$, it means the critical moment is larger than the Brazier moment due to the restraint of ovalization by the boundary conditions. It can also be noted that for long cylinders with Brazier critical ovalization, the dimensionless curvature k' at critical load is larger than 1, which is due to the reduced tangential modulus during deformation caused by geometric nonlinearity, but ϕ_{Braz} is obtained regarding the linear bending hypothesis.

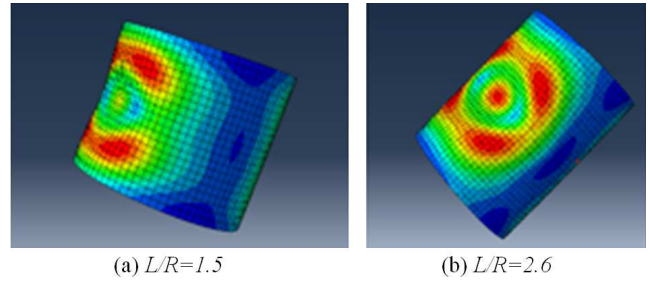


Figure 3. The buckling mode for short cylindrical shells.

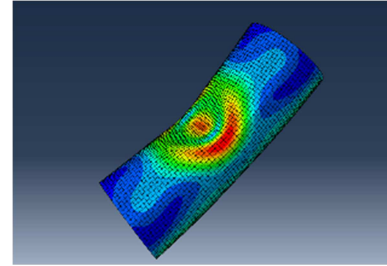


Figure 4. The buckling mode for medium long cylindrical shells $L/R=5$.

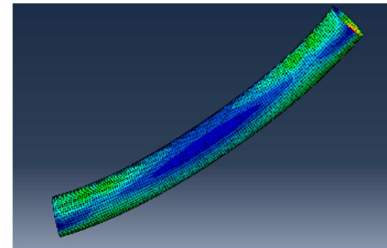


Figure 5. The buckling mode for long cylindrical shells $L/R=18$.

2.4. Maximum Critical Bending Moment Prediction

The results of this method are shown in Figures 6 and 7. The results can be divided into a range. When the shell is relatively short, there is minimal ovalization of the shells as the bending moment increases, and there is local buckling at the end. The shorter the shell, the easier it is for local buckling to occur.

As a result, the dimensionless moment k_1 decreases as the shell length increases to the extent shown in Figure 6. When the radius shrinks, the dimensionless moment also decreases.

Figure 3 shows the buckling mode when the shell is relatively short.

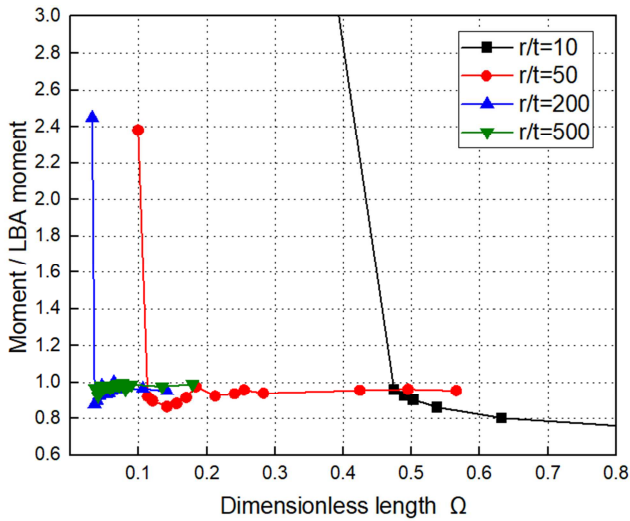


Figure 6. Relation between dimensionless moment k_1 and dimensionless length.

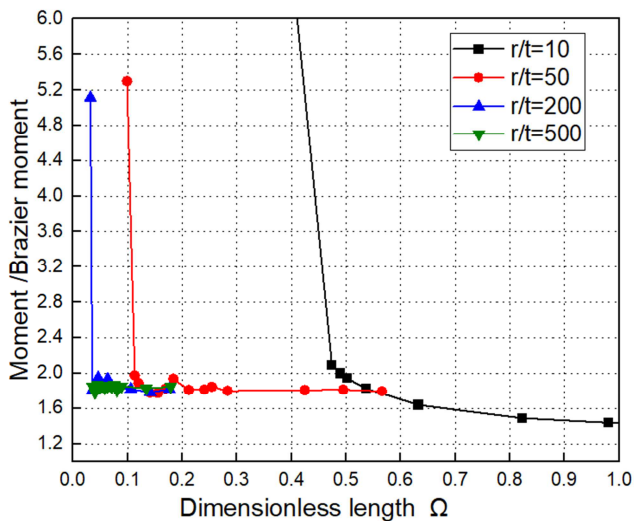


Figure 7. Relation between dimensionless moment k_2 and dimensionless length.

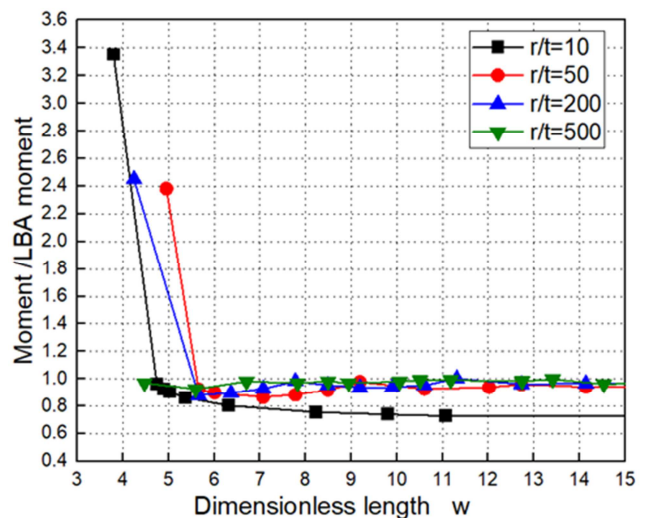
The ovalization and buckling of the shell both have an effect on critical strength. With increasing length, the ovalization rises at the point of local buckling, and the boundary moment gradually shifts toward the Brazier moment. The local buckling point is moved to the shell's center. Buckling strength is reduced when the shell is very thick, for example, $R/t=10$ and 50, but almost the same when R/t is equal to 200 and 500 (maybe longer). Figure 4. depicts a buckling mode for medium-length shells.

Finally, the limiting moment slowly decreases toward a minimum value. When the shell is longer than the limiting moment, the dimensionless moment becomes somewhat longer owing to the change in buckling mode and the local buckling point is shifted from the center of the shell to the two ends. The thinner shells have a lower buckling strength rating. The buckling mode for long shells is illustrated in Figure 5.

Figure 6 describes the connection and the behaviour among the dimensionless crucial moment k_1 and dimensionless length for medium and long tubes. A mixture of ovalization and bifurcation uncertainty happens in a range of $0.5 \leq \Omega \leq 1$ on $R/t=10$. With increasing Ω , the elastic critical moment decreases progressively, and the number of ovalization of the cross-sectional in the region where the buckle occurs as well. The crucial moment decreases continuously as Ω increases towards a persistent value to an indefinitely long cylinder. Meanwhile, at $R/t=50$, the same range is constant.

At the critical bending moment, the limit among medium-length tubes with incomplete ovalization of the cross-section and long tubes with Brazier crucial ovalization of cross-sectional can be defined approximately at $0 \leq \Omega \leq 0.1$ for $R/t=200$ and 500, then at $0.1 \leq \Omega \leq 0.2$ for $R/t=50$, and $\Omega=0.5$ for $R/t=10$. Details of the curves are illustrated in Figure 7, where k_2 replaces the dimensionless moment parameter k_1 . For long tubes with Brazier crucial ovalization, k_2 's value is less than 2.1, suggesting that the M_{cr} is somewhat small compare to M_{Braz} . The dimensionless moment k_2 with Brazier critical ovalization stabilizes between 1.7 and 1.9 for $R/t \geq 50$. Comparable number for thicker tubes is somewhat less than 1.5 (1.42 for $R/t=10$). This is because of two factors; Firstly, the M_{GNA} determined is the crucial value at the bifurcation buckling point, which usually happens after M_{Braz} . Secondly, k_2 is a bit affected by R/t . It is actually because of the influence of geometrical nonlinearity in the pre-buckling stage which varies somewhat with R/t .

The bending effect towards the ends soon decays with a minor increase in L/R (Figure 3b). The most compressed fiber is at the center of the material, resulting in local bifurcation buckling, which influences the buckle behavior. However, the half wavelength of the axial buckling remains lengthy, and bifurcation buckling is still limited by the boundaries. The buckling stress necessite to generate an axial compressive buckle which is a little more than the normal value for medium-length tubes under pure bending that is self reliant of the boundary conditions. The center of the shell experiences bifurcation buckling for $L/R=2.6$.



(a)

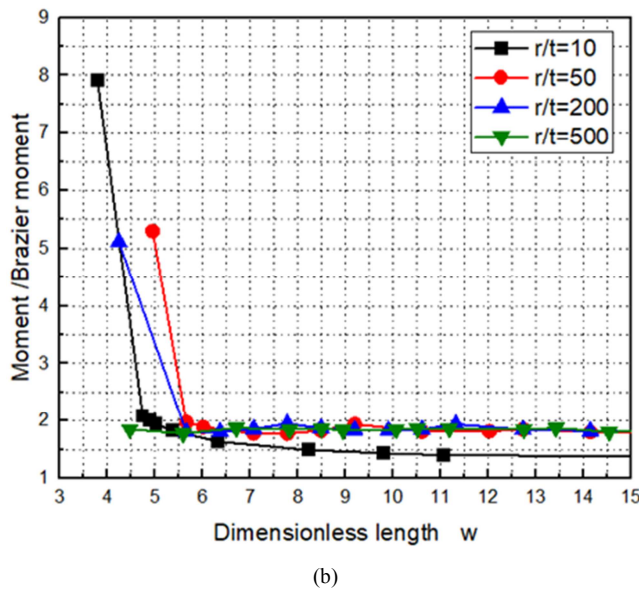


Figure 8. Relationship between the dimensionless moment k_1 (a) then k_2 (b) and the length parameter ω .

Figure 8 illustrate the details for short cylinders. When the extent lengthwise is represented according to the dimensionless length parameter ω , the relation of the critical moment-length curves for short cylinders with varied r/t values are similar. k_1 and k_2 's value grow rapidly with decreasing length for exceedingly short cylinders. This is due to the limits considerably restricting the buckling formations on the tubes, hence increasing the crucial bending moment dramatically.

When the tube's extend lengthwise is not too tiny then falls into an average range, k_1 's value approaches one, indicating that the geometrical nonlinear elastic analysis critical bending moment is near M_{cr} (critical buckling moment) [16]. In this analysis, cylinders with a range of $100 < r/t < 1000$ were examined and the conclusion that the essential bending stress for quite tiny cylinders is not more than 10% more than that for pure compression was made.

The fluctuating connection among the size of the cylindrical shell and the wavelength's buckle is responsible for this phenomenon. Most values of k_1 are significantly less than 1 for thin cylindrical shell with $r/t \geq 50$ on an interval of $6 < \omega < 10$ (Figure 8a). This decrease is due to the minor effect of geometric nonlinearity generated by bending on the buckling strength M_{GNA} because M_{cr} is computed using the linear bending theory of shells without taking geometric nonlinearity into account. As L/r increases, the value at which the ovalization of the cross-section begins to affect buckling behavior varies according to r/t .

From a fairly modest value of ω on short tubes with $r/t = 10$, the buckling strength start changing. The value of ω where the oval distortion begins to impact on the buckling behavior of tubes subjected to global bending is specified here as a border among tiny and medium extent lengthwise tubes.

3. Conclusion

The numerical nonlinear stability analysis of elastic

strength steel tubes under global bending with various dimension was investigated. And we realized that in the tiny tubes mostly in their center, some bifurcation occurred more on the bending location. We also observed negligible ovalization, and GNA analysis critical bending moment is near to M_{cr} . Because of the constraint provided by the boundary conditions, local snap-through buckling along the borders occurs for extremely short cylinders, causing the critical bending moment to climb to several times M_{cr} . Then for medium-length tubes, it was observed that both ovalization and bifurcation instability occurred. The importance of cross-sectional ovalization should be stressed since its result could be significant to a reduction in elastic buckling stress under values of homogeneous axial compression. Longer tubes exhibit more evident ovalization during pre-buckling stage, resulting in an interesting depletion in critical bending moment. Bifurcation buckling occurs soon before snap-through buckling in long tubes, and the two buckling points are nearly indistinguishable. With Brazier critical ovalization of the cross sectional, the critical moment is 64, which is almost equivalent to the Brazier moment.

References

- [1] Antoine, P. A., 2000. Comportement des coques cylindriques minces sous chargements combinés: vers une amélioration du dimensionnement sous flexion et pression interne. (Behavior of thin cylindrical shells under combined loading: towards an improved design process for bending and internal pressure), Ph.D. thesis, INSA de Lyon, Lyon, France.
- [2] Flugge, W., 1973. Stresses in Shells, second ed. Springer-Verlag, Berlin.
- [3] Hibbitt, D., Karlsson, B., Sorensen, P.: ABAQUS Version 6.6 Standard user's guide and theoretical manual. HKS Inc., Pawtucket, Rhode Island, USA, 2006.
- [4] Stephens, W. B., Starnes Jr., J. H., 1975. Collapse of long cylindrical shells under combined bending and pressure loads. AIAA J. 13 (1), 20-25.
- [5] Russell, P. and Dowell, G. (1933) Competitive Design of Steel Structures. London: Chapman & Hall, Ltd. Seide, P., Weingarten, V. I.: On the Buckling of Circular Cylindrical Shells Under Pure Bending. Journal of Applied Mechanics, 28 (1961), pp. 112–116.
- [6] Bjorhovde, R. (2004) Development and use of high-performance steel. Journal of Constructional Steel Research, 60: 393–400.
- [7] Brazier, L. G.: On the flexure of thin cylindrical shells and other 'thin' sections. Proceedings, Roy. Soc. London Series A, 116 (1927), pp. 104–114.
- [8] Von Kármán, T., 1911. Über die Formänderung dünnwandiger Rohre, insbesondere federnder Ausgleichsrohre. VDI-Zeitschrift 55, 1889–1895.
- [9] C. R. Calladine: Theory of Shell Structures, Cambridge University Press, Cambridge (1983).

- [10] E. L. Axelrad: Refinement of buckling-load analysis for tube flexure by way of considering precritical deformation, [in Russian] *Izvestiya Akademii Nauk SSSR, Otdelenie Tekhnicheskikh Nauk, Mekhanika i Mashinostroenie* (1965), Vol. 4, p. 133-139.
- [11] Hibbit, Karlsson, Sorensen, 1998. *ABAQUS /Standard Theory and User's Manuals*.
- [12] Riks, E., Rankin, C. C., Brogan, F. A., 1996. On the solution of mode jumping phenomena in thin-walled shell structures. *Comput. Methods Appl. Mech. Engng.* 136, 59–92.
- [13] Rotter, J. M., 2004. Buckling of cylindrical shells under axial compression. In: Teng, J. G., Rotter, J. M. (Eds.), *Buckling of Thin Metal Shells*. Spon Press, London, pp. 42–87.
- [14] Almroth, B. O., Starnes Jr., J. H., 1973. The computer in shell stability analysis. In: Presented at the 1973 ASCE National Structural Engineering Meeting, San Francisco.
- [15] Teng, J. G., Song, C. Y., 2001. Numerical models for nonlinear analysis of elastic shells with eigenmode-affine imperfections. *Int. J. Solids Struct.* 38 (18), 3263–3280.
- [16] Seide, P., Weingarten, V. I., 1961. On the buckling of circular cylindrical shells under pure bending. *J. Appl. Mech., ASME* 28 (1), 112– 116.